Mon. Not. R. astr. Soc. (1990) **243**, 276–281

Tidal change in the energy of a spherical galaxy

P. M. S. Namboodiri and R. K. Kochhar
Indian Institute of Astrophysics, Bangalore 560034, India

Accepted 1989 September 11. Received 1989 September 11; in original form 1989 May 21

SUMMARY

Tidal effects of a massive perturber on a satellite galaxy have been studied by numerical simulations. The model consists of a spherical satellite galaxy and a point-mass perturber and the encounter is non-penetrating. A wide range of density ratios and eccentricities of the orbit have been used. The disruption of the satellite galaxy has been observed when the numerical value of the fractional change in the energy is greater than two. The energy change shows smooth variation with time in the case of unbound orbits and irregular variation in the bound orbit cases. It is shown that, for a constant pericentric distance, increasing the density ratio decreases the tidal effects, and for a given density ratio an increase in the eccentricity decreases the tidal effects. N-body results are compared with predictions of analytical estimates.

1 INTRODUCTION

Tidal disruption and merger are two important processes in the dynamical evolution of a binary stellar system. The merger time of two galaxies of comparable mass is shorter than the disruption time. On the other hand, a massive primary is likely to cause considerable disruption of the satellite and, in this case, the disruption time could be shorter than the merger time.

Many earlier simulations dealt mainly with collisions of galaxies of comparable mass (van Albada & van Gorkom 1977; White 1978; Gerhard 1981; Farouki & Shapiro 1982; Negroponte & White 1983; Lin & Tremaine 1983; Barnes 1988). Collisions of galaxies of unequal masses were considered by Dekel, Lecar & Shaham (1980), Villumsen (1982), Aguilar & White (1985) and Rao, Ramamani & Alladin (1987). Villumsen (1982) concentrated on mergers while Dekel *et al.* (1980) considered slow hyperbolic encounters and obtained total changes in the energy. Aguilar & White (1985) also considered hyperbolic encounters and compared their N-body results of energy change and mass loss with impulse approximation estimates as expected from Spitzer's (1958) theory. They found reasonable agreement between the two cases. Rao *et al.* (1987) compared their numerical results with impulse approximation estimates and found agreement for orbital eccentricity $e \geq 0.5$.

Miller (1986) considered the tidal effects of a galaxy orbiting in a cluster of galaxies in a highly eccentric orbit and derived the criterion for disruption. From a comparison between analytic results of impulse approximation (IA) and adiabatic approximation (AA), Alladin, Ramamani & Meinya Singh (1985) had suggested that, for density of the satellite much greater than the Roche density ρ_R, the tidal effects would be greater for a parabolic orbit than for a circular orbit, whereas for $\rho \approx \rho_R$ the reverse would be the case. In order to test this statement numerically we have carried out N-body simulations of non-penetrating stellar systems over a wide range of density ratio and eccentricity e. We have extended the work of Rao *et al.* (1987) to include also the circular cases. We have also determined the fractional changes in the mass loss and energy in each case and compared them with analytical estimates.

2 METHOD AND INITIAL CONDITIONS

2.1 The method

We consider two model galaxies of which the more massive one is a point mass and called the primary (or the perturber); and the less massive, the satellite (or the test galaxy). The mass of the test galaxy is denoted by M and that of the primary by M_1. The test galaxy is a spherical cluster of 250 particles. The motion of the individual particles is governed by the equation

$$\frac{d^2\mathbf{r}_1}{dt^2} = -G\sum_{\substack{j=1\\ j\neq i}}^{N} \frac{m_j \mathbf{r}_{ij}}{r_{ij}^3}, \quad i = 1, 2, 3, \ldots N, \tag{1}$$

where $\mathbf{r}_i$ is the position vector of the i^{th} particle in an inertial frame of reference, m_i its mass, $\mathbf{r}_{ij} = \mathbf{r}_i - \mathbf{r}_j$, G is the gravitational constant, N is the number of particles and t is the time. We use a softened potential for each particle, given by

$$\phi_i = -G\sum \frac{m_j}{(r_{ij}^2 + \varepsilon^2)^{1/2}}, \tag{2}$$

where ε is the softening parameter. The integration of the

orbit of each particle is accomplished using Aarseth's N-BODY2 code. For details of the integration procedure see Ahmed & Cohen (1973).

2.2 Initial conditions

We use a system of dimensionless units in which $G=1$. The particles in the test galaxy are each given unit mass and are distributed within a sphere of radius $R=20$ units. If we take $R=20$ kpc and $M=10^{11}M_{\odot}$, the unit of time is nearly equal to 1.3×10^{8} yr and the unit of velocity is 147 km s^{-1}. The initial mass-distribution follows the law $M(r)\propto r$. The softening parameter has been taken as $\varepsilon=0.1R$. Each particle is initially given a velocity equal to the circular velocity appropriate to its position, and the directions of the velocity vectors are chosen randomly. The cluster so formed is very close to virial equilibrium. Its half-mass radius R_h is nearly equal to 10 units with $V_{rms}=2.6$ and a crossing time close to eight time units. The test galaxy has initially no net angular momentum.

The test galaxy is evolved for about eight crossing times to obtain a dynamically stable system. The parameters of the initial system and the evolved one (standard model) are given in Table 1. The evolved system shows a higher concentration toward the centre and expansion in the outer region; 90 per cent of its mass is within about $3R_h$ (denoted by $R_{0.9}$) and the radius of the total system (denoted by R_B) extends to about $6R_h$. The standard model is used as the initial galaxy for subsequent encounters with another galaxy.

Several experiments are performed to study the tidal effects of the primary on the satellite. The initial separation r_0 of the two galaxies is chosen such that $r_0=kp$, where p is the distance of closest approach associated with the initial Kepler orbit. The values of k used are given in Table 2 column 4. The orbital plane of M_1 is chosen to be the X–Y plane with the X-axis pointing in the direction of closest approach. The initial relative velocity of M_1 appropriate to

Table 1. Parameters of the initial and evolved systems.

MODEL	R_h	R_B	$R_{0.9}$	R_{rms}	V_{rms}	V_{Disp}	V_{rrms}/V_{trms}
INITIAL	10.25	19.75	18.03	11.73	2.60	0.97	0.66
STANDARD	6.55	36.62	18.62	10.81	3.42	1.45	0.74

Note: R_h is the half-mass radius; R_B the radius of the bound part; $R_{0.9}$ is the radius containing 90 per cent of the mass; R_{rms} and V_{rms} are, respectively, the root mean square radius and velocity; V_{disp} is the velocity dispersion; V_{rrms} and V_{trms} are the root mean square values of radial and tangential velocity.

Table 2. Collision parameters and results of encounter.

MODEL	ρ_h/ρ_R	M_1/M	r_0/p	V_P/V_{rms}	$\Delta U/\lvert U\rvert$	$\Delta U/\lvert U\rvert_{AN}$	$\Delta U/\lvert U\rvert_{Sp}$	$\Delta U_B/\lvert U\rvert$	$\Delta M/M$
H1	0.75	1186.2	3.0	27.591	2.080	3.334	2.631	0.716	0.420
H2	1.50	593.1	3.0	19.518	1.260	1.666	1.315	0.576	0.316
H3	2.67	333.3	3.0	14.641	0.986	0.934	0.738	0.450	0.260
H4	5.34	166.7	3.0	10.370	0.514	0.466	0.368	0.265	0.148
P1	0.75	1186.2	2.0	22.528	6.203	7.304	3.947	0.956	0.812
P2	1.50	593.1	2.0	15.936	5.357	3.649	1.972	0.771	0.548
P3	2.67	333.3	2.0	11.954	4.100	2.048	1.107	0.594	0.388
P4	5.34	166.7	2.0	8.467	2.297	1.021	0.552	0.403	0.272
P5	10.68	83.3	2.0	6.003	0.970	0.507	0.274	0.209	0.124
P6	21.36	41.7	2.0	4.272	0.449	0.251	0.136	0.131	0.068
P7	42.71	20.8	2.0	3.053	0.066	0.122	0.066	0.037	0.024
P8	85.41	10.4	2.0	2.209	0.051	0.059	0.032	0.024	0.008
P10	341.63	2.6	2.0	1.241	0.003	0.012	0.006	0.003	0.000
E1	0.75	1186.2	1.5	19.510	14.095	17.313	5.263		1.000
E2	1.50	593.1	1.5	13.801	13.222	8.650	2.629		1.000
E3	2.67	333.3	1.5	10.353	10.236	4.854	1.475		1.000
E4	5.34	166.7	1.5	7.333	8.711	2.420	0.736	0.514	0.396
E5	10.68	83.3	1.5	5.199	3.774	1.202	0.365	0.290	0.236
E6a	21.36	41.7	3.0	3.700	1.035	0.595	0.181	0.168	0.140
E6b					1.754			0.227	0.196
E7a	42.71	20.8	3.0	2.644	0.396	0.290	0.088	0.089	0.076
E7b					0.838			0.152	0.156
ESa	33.21	10.0	9.0	2.424	0.248	0.205	0.090	0.111	0.080
ESb					0.574			0.185	0.188
C6	21.36	41.7	1.0	3.021	11.470	2.008	0.271		1.000
C7	42.71	20.8	1.0	2.159	1.610	0.978	0.132	0.196	0.172
C8a	85.41	10.4	1.0	1.561	0.553	0.467	0.063	0.093	0.084
C8b					0.539			0.159	0.128
C10a	341.63	2.6	1.0	0.878	0.032	0.093	0.013	0.024	0.016
C10b					0.062			0.050	0.036

Note: Column 1: The model used: hyperbolic (H), parabolic (P), elliptic (E), and circular (C); the number following the letter indicates the density ratio (see text), 'a' indicates the first encounter and 'b' the second; column 2: density ratio; column 3: mass ratio; column 4: initial separation in terms of p; column 5: V_p/V_{rms}, V_p is the velocity at closest approach; columns 6, 7, 8: fractional change in the energy obtained from N-body results, IA (Alladin & Narasimhan), and IA (Spitzer); column 9: fractional energy of the bound part: column 10: fractional mass loss.

its distance r_0 is determined from the standard point-mass formula.

The positions and velocities of the particles in the test galaxy and of the perturber were recalculated with reference to the centre-of-mass frame of the total system. The evolution of the test galaxy had been followed until the perturber reached a distance $r > 2p$. In some bound orbit cases the integration was performed for two orbital periods.

3 NUMERICAL RESULTS

We consider four models in which the perturber is allowed to move in hyperbolic (model H), parabolic (model P), elliptic (model E) and circular (model C) orbits. Out of the 25 simulations reported here, four are hyperbolic, nine parabolic, eight elliptic and four circular encounters. In all but one model the distance of closest approach, p, is 100. In hyperbolic encounters, the primary is assumed to move in an orbit of eccentricity $e = 2$, whereas in the elliptic case $e = 0.5$. These values of p and e are meaningful only if the galaxies are assumed to be point masses moving in Keplerian orbits. It should, however, be noted that soft potential orbits are not conical orbits and our use of p and e is meaningful only to a good approximation but not strictly (Gerhard 1981; White 1978). The mean density ρ_h of M within a sphere of radius R_h is

$$\rho_h = \frac{M/2}{4/3\pi R_h^3}. \tag{3}$$

The Roche density ρ_R is defined as

$$\rho_R = 2\rho_1 = 2\left(\frac{3M_1}{4\pi p^3}\right). \tag{4}$$

We consider density ratios $\rho_h/\rho_R = 0.75$, 1.50, 2.67, 5.34, 10.68, 21.36, 42.71, 85.41, 341.63 and these are denoted by the numbers 1, 2, 3, 4, 5, 6, 7, 8 and 10. For model ES we use $\rho_h/\rho_R = 33.21$, $e = 0.8$ and $p = 72$. In models E6, E7, ES, C8 and C10 the evolution of the satellite has been followed for two orbital periods.

The results of the simulations are stored at specified time intervals. The centre-of-mass of N particles (excluding the perturber) is computed at each time interval and particles with positive energy with respect to this centre-of-mass are identified as escapers. The centre-of-mass of the remaining particles is again evaluated and the escapers relative to this new centre-of-mass are identified next. This procedure is continued until convergence is reached. In this way we arrive at the number of escapers, the number of bound particles with respect to the test galaxy, and the energy U_B of the bound part (see Dekel *et al.* 1980). The collision parameters as well as the results for energy change and mass loss are given in Table 2.

4 DISCUSSION

4.1 General features

Tidal damage is seen to occur after the perturber has passed the closest approach point. The tendency to form bridges and tails is observed when the perturber is near the closest approach distance. As the perturber recedes, the bridges collapse but tails survive for longer duration as indicated by Toomre & Toomre (1972). The central regions became more compact as a result of the encounter. This would increase the surface brightness of the satellite as discussed by Faber (1973) and Byrd (1987). Total disruption is observed in models P1, P2, E1, E2, E3 and C6. Disrupted galaxies generally appear amorphous with no well-defined centre.

4.2 Mass loss

Mass loss and energy change in various models are shown in Figs 1–4. The variation of $\Delta M/M$ with time is shown by dotted lines in Figs 1 and 2, and by open circles in Figs 3 and 4. Here $\Delta M = M - M_B$, where M_B is the mass of the final bound system. The percentage of mass loss is almost 40 or more in models H1, P1–P3, E1–E4 and C6. In these models

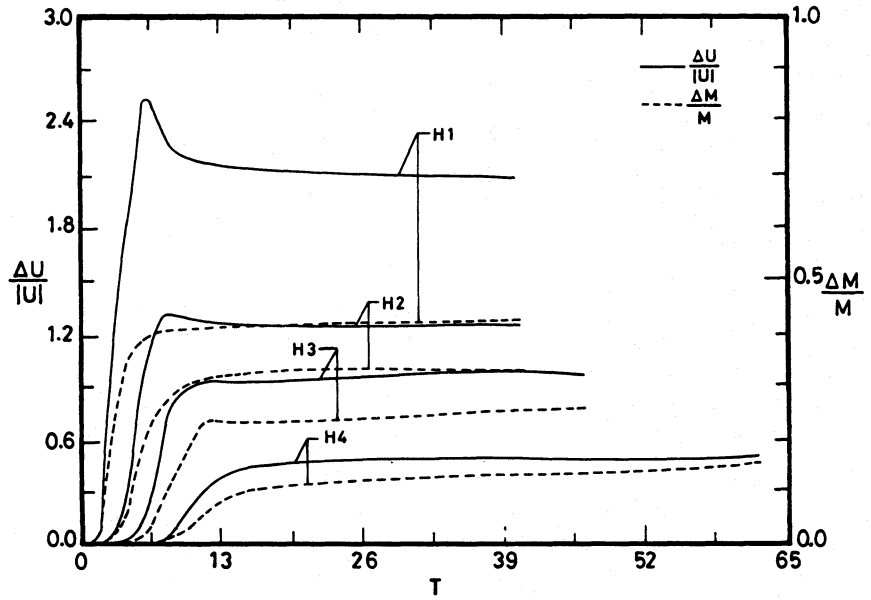

Figure 1. Fractional change in energy and mass loss as a function of time T for H models.

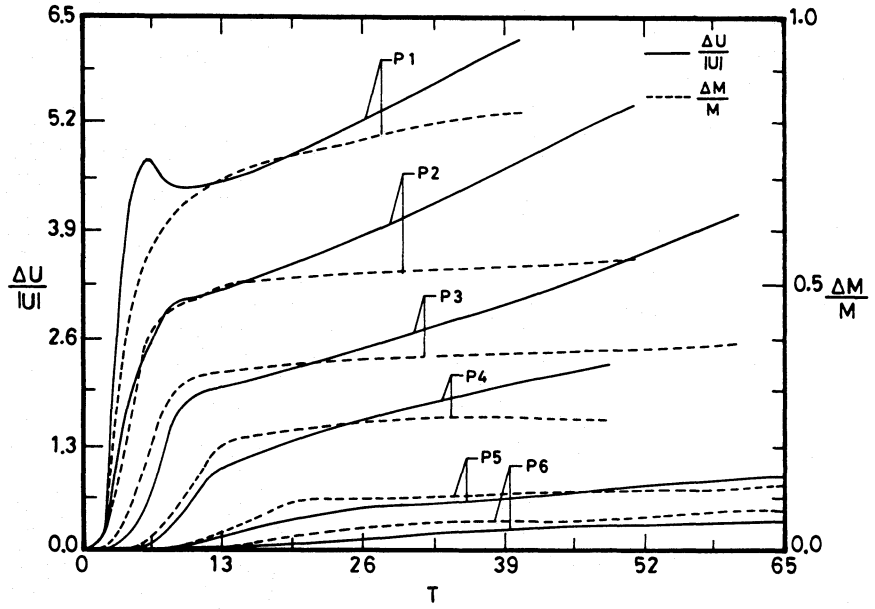

Figure 2. Same as Fig. 1, but for P models.

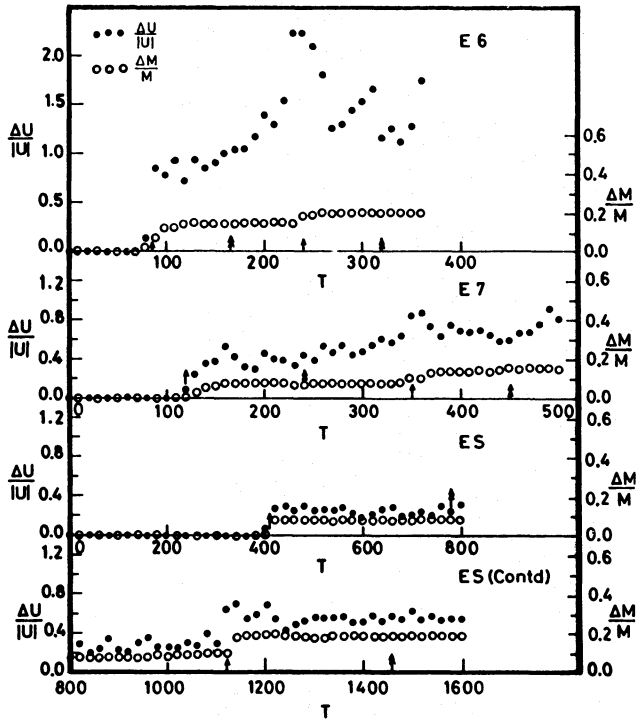

Figure 3. Same as Fig. 1, but for models E6, E7 and ES. Symbols ↑ and ↕, respectively indicate times of minimum and maximum separation.

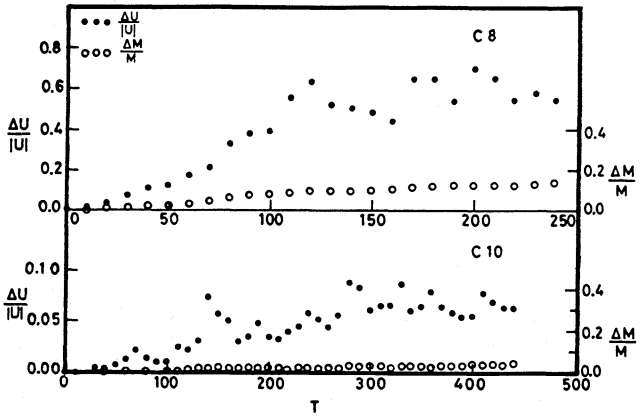

Figure 4. Same as Fig. 1, but for models C8 and C10.

the test galaxy is either completely or significantly disrupted. Miller (1986) has pointed out that disruption occurs when mass loss exceeds 30 or 40 per cent. He performed computations with 60 000 particles in a galaxy orbiting within a cluster and obtained the strength of the interaction in terms of the ratio of the maximum tidal force F_T and the internal force F_I at median radius of the satellite. Miller's condition for a galaxy not to be disrupted is $F_T/F_I < \frac{1}{4}$. The ratio F_I/F_T is nearly equivalent to the density ratio ρ_h/ρ_R and thus disruption occurs when $\rho_h/\rho_R < 4$ which is in conformity with Miller's result. It can be seen from Figs 3 and 4 that in models E6, E7, ES, C8 and C10 the mass loss reaches a maximum during the first close contact; it is negligible and remains nearly constant during the subsequent encounter.

4.3 Energy transfer

The energy gained by the stars in the satellite during an encounter is a measure of the damage done to it. We plot the fractional change in the energy of the system $\Delta U/|U|$ as a function of time by solid lines in Figs 1 and 2, and by filled circles in Figs 3 and 4. Here $\Delta U = U_f - U$, where U_f is the final energy of the satellite including escapers and U is the unperturbed initial energy of the satellite. Ideally one should use energy per unit mass of the test galaxy (Binney & Tremaine 1987). But, since we are dealing with ratios, the quantity we use is the total energy. In all models, most of the change in the energy occurs after the perturber crosses the perigalactic point. In H- and P-models, the change in the

energy remains nearly constant after this instant, provided there is no disruption. In disruptive cases the energy of the satellite continues to increase. This is observed in models P1–P3 and E1–E5.

In unbound encounters the variation of $\Delta U/|U|$ with time is smooth. This is because the perturber is always on one side of the satellite as a result of which the satellite continuously gains energy. The amount of energy transferred decreases monotonically as the perturber moves away from the satellite. On the other hand, in models E6, E7, ES, C8 and C10 the satellite's energy shows irregular variation with time. This is because, in these models, the perturber is moving in closed orbit as a result of which the direction of tidal acceleration gets partially reversed. The energy changes reach a maximum at the close contact point. Slight enhancement in the energy is observed when the perturber makes a second close contact.

4.4 Comparison with predictions of analytical formulae

In this section we compare our results with analytical estimates obtained using impulse approximation (IA). For a conic orbit of eccentricity e the following relations have been obtained under IA (Alladin & Narasimhan 1982; Narasimhan & Alladin 1983). These will be denoted by the subscript AN.

$$\left(\frac{\Delta U}{|U|}\right)_{\mathrm{AN}} = \frac{2\pi^2}{(1+e)^2}\frac{G^2M_1^2}{p^4V_{\mathrm{p}}^2}\left(R_{\mathrm{rms}}/V_{\mathrm{rms}}\right)^2,\ e\le 1, \tag{5}$$

$$\left(\frac{\Delta U}{|U|}\right)_{\mathrm{AN}} = (1+e)\langle e_i^2\rangle\frac{G^2M_1^2}{p^4V_{\mathrm{p}}^2}\left(R_{\mathrm{rms}}/V_{\mathrm{rms}}\right)^2,\ e>1, \tag{6}$$

where $\langle e_i^2\rangle$ is a complicated function of e and is given by Narasimhan & Alladin (1983). Rao *et al.* (1987) have shown that IA estimates given by equations (5) and (6) agree with numerical results for $e\ge 0.5$. We have extended the calculations to include also the circular orbit and we find that the values of $\Delta U/|U|$ given by equation (5) agree with our numerical results within a factor of 2. In Fig. 5 we plot the variation of $\log(\Delta U/|U|)$ versus $\log(\rho_{\mathrm{h}}/\rho_{\mathrm{R}})$. The dotted lines show the curves for IA values. The agreement between the numerical results and the IA estimates is very good in the H-models as noted by earlier workers. The validity of the formulae becomes less accurate as one decreases the eccentricity of the perturber's orbit. Nevertheless the IA estimates agree with numerical results within a factor of 2 in the range $0.1<\Delta U/|U|<2$. The IA underestimates the tidal effects when $\Delta U/|U|>2$, whereas it overestimates them when $\Delta U/|U|<0.1$. This is due to the fact that for $\Delta U/|U|>2$ there is much loosening of the test galaxy which enhances the tidal effects, whereas for $\Delta U/|U|<0.1$ the motion of the stars reduces the tidal effects and these factors are not taken into account in the IA. In the range of validity of the formulae the two opposite effects nearly balance each other. Disruption occurs if $\Delta U/|U|>2$ as earlier indicated by Miller (1986). This is nearly equivalent to $\rho_{\mathrm{h}}/\rho_{\mathrm{R}}<4$ except in H-models, where its value is slightly less for disruption. For fast encounters we can obtain from Spitzer's theory

$$\left(\frac{\Delta U}{|U|}\right)_{\mathrm{Sp}} = \frac{8}{3}\frac{G^2M_1^2}{p^4V_{\mathrm{p}}^2}\left(R_{\mathrm{rms}}/V_{\mathrm{rms}}\right)^2. \tag{7}$$

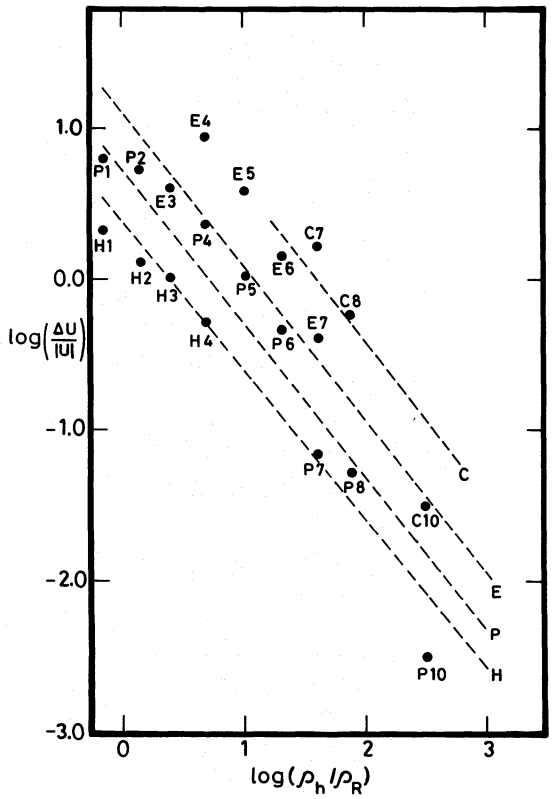

Figure 5. Variation of $\log(\Delta U/|U|)$ with $\log(\rho_{\mathrm{h}}/\rho_{\mathrm{R}})$ for all the models. The dashed lines show the results obtained from impulse approximation calculation

The values of $\Delta U/|U|$ obtained using equations (5)–(7) are given in Table 2 in columns 6 and 7, respectively. It can be seen that Spitzer's formula is valid for H-models.

Table 3 shows the values of $\Delta U/|U|$ for various eccentricities and density ratios. Recall that $\Delta U/|U|>2$ means disruption. At places we have used the symbols D and ND to, respectively, denote disruption and non-disruption. It can be seen from Table 3 that increasing the density ratio $\rho_{\mathrm{h}}/\rho_{\mathrm{R}}$ decreases the tidal effects, and for a given density ratio, increasing the orbital eccentricity decreases the tidal effects. If we compare, for example, the tidal effects in the parabolic and circular cases we find that the ratio, $(\Delta U/|U|)_{\mathrm{parabolic}}/(\Delta U/|U|)_{\mathrm{circular}}$, decreases with increasing $\rho_{\mathrm{h}}/\rho_{\mathrm{R}}$ whereas the

Table 3. Values of $\Delta U/|U|$

$\rho_{\mathrm{h}}/\rho_{\mathrm{R}}$ \ e	0	0.5	1	2
0.75	D	14.095	6.203	2.080
1.50	D	13.222	5.357	1.260
2.67	D	10.236	4.100	0.986
5.34	D	8.711	2.297	0.514
10.68	D	3.774	0.970	ND
21.36	11.470	1.035	0.449	ND
42.71	1.610	0.396	0.066	ND
85.41	0.553	ND	0.051	ND
341.63	0.032	ND	0.003	ND

IA does not suggest this. This is in agreement with the suggestion made by Alladin *et al.* (1985) from a comparison of the results of IA and AA that, for large density of the satellite, the parabolic case would give greater energy transfer than the circular case. Although the tendency of our results is in this direction we find that this limit has not been reached until $\Delta U/|U| \approx 0.01$. It remains to be confirmed numerically whether this would happen at still lower values of $\Delta U/|U|$.

Alladin *et al.* (1985) have also shown that there would be a sharp decrease in the disruption rate at $\rho_h \approx \rho_R$. The numerical work does not support this. On the contrary we find that the variation of $\Delta U/|U|$ with ρ_h/ρ_R is smooth over a wide range of density ratios which includes $\rho_h/\rho_R = 1$. King's (1962) formula for tidal radius R_t

$$R_t = p\left(\frac{M}{M_1(3+e)}\right)^{1/3} \tag{8}$$

suggests that tidal effects depend weakly on e and increase with e if p and masses of the galaxies are kept constant. But the numerical work shows that the tidal effects decrease with increasing e, and depend on e if the density ratio and the distance of closest approach are kept constant.

5 CONCLUSIONS

We have used self-consistent N-body simulations to study the energy transfer and mass loss of a spherical galaxy due to the tidal effects of a perturbing galaxy for various density ratios ρ_h/ρ_R and eccentricity e of the perturber's orbit. The main conclusions are as follows.

(i) Disruption of a satellite galaxy occurs (i.e. the satellite galaxy loses more than 40 per cent of its mass) if the value of $\Delta U/|U|$ is greater than 2.

(ii) Most of the change in $\Delta U/|U|$ occurs after the perturber passes the closest approach point; the change in the energy in the second half is larger by a factor of 2 than the corresponding change in the first half.

(iii) The impulse approximation estimates of $\Delta U/|U|$ as given by equations (5) and (6) agree within a factor of 2 with numerical results for all eccentricities, in the range $0.1 < \Delta U/|U| < 2$. For $\Delta U/|U| < 0.1$ these formulae overestimate the energy transfer due to the neglect of stellar motions and for $\Delta U/|U| > 2$ they underestimate the same due to the neglect of the loosening of the satellite.

(iv) The fractional change in the energy of the satellite galaxy shows smooth variation in hyperbolic and parabolic encounters and irregular variation in elliptic and circular encounters; this is due to the partial reversal of the direction of the tidal acceleration during a part of the orbit in the latter case.

(v) The tidal effects increase with decreasing eccentricity e for constant ρ_h/ρ_R and p. It remains to be investigated whether the opposite holds for values of ρ_h/ρ_R larger than those we have used.

Conclusions (i) and (ii) have been obtained earlier by several workers for collisions of galaxies of comparable mass. We confirm these results over a wide range of the density of the satellite and eccentricity of the orbit. Conclusions (iii), (iv) and (v) appear to be new.

ACKNOWLEDGMENTS

We thank Drs S. M. Alladin, for many useful discussions, and S. J. Aarseth for kindly making his N-body codes available to us. We also thank the referee Dr J. J. Binney for criticism.

REFERENCES

Aguilar, L. A. & White, S. D. M., 1985. *Astrophys. J.*, **295,** 374.
Ahmed, A. & Cohen, L., 1973. *J. Comput. Phys.*, **12,** 389.
Alladin, S. M. & Narasimhan, K. S. V. S., 1982. *Phys. Rep.*, **92,** 339.
Alladin, S. M., Ramamani, N. & Meinya Singh, T., 1985. *Astr. Astrophys.*, **6,** 5.
Barnes, J. E., 1988. *Astrophys. J.*, **331,** 699.
Binney, J. J. & Tremaine, S., 1987. *Galactic Dynamics,* Princeton Series in Astrophysics.
Byrd, G. G., 1987. In: *The Few Body Problem,* p. 371, ed. Valtonen, M. J., Kluwer, Dordrecht.
Dekel, A., Lecar, M. & Shaham, J., 1980. *Astrophys. J.*, **241,** 946.
Faber, S. M., 1973. *Astrophys. J.*, **179,** 423.
Farouki, R. T. & Shapiro, S. L., 1982. *Astrophys. J.*, **259,** 103.
Gerhard, O. E., 1981. *Mon. Not. R. astr. Soc.*, **197,** 179.
King, I. R., 1962. *Astr. J.*, **67,** 41.
Lin, D. N. C. & Tremaine, S., 1983. *Astrophys. J.*, **264,** 364.
Miller, R. H., 1986. *Astr. Astrophys.*, **167,** 41.
Narasimhan, K. S. V. S. & Alladin, S. M., 1983. *Bull. astr. Soc. India,* **11,** 221.
Negroponte, J. & White, S. D. M., 1983. *Mon. Not. R. astr. Soc.*, **205,** 1009.
Rao, P. D., Ramamani, N. & Alladin, S. M., 1987. *Astr. Astrophys.*, **8,** 17.
Spitzer, L., 1958. *Astrophys. J.*, **127,** 17.
Toomre, A. & Toomre, J., 1972. *Astrophys. J.*, **178,** 623.
van Albada, T. S. & van Gorkom, J. H., 1977. *Astr. Astrophys.*, **54,** 121.
Villumsen, J. V., 1982. *Mon. Not. R. astr. Soc.*, **199,** 493.
White, S. D. M., 1978. *Mon. Not. R. astr. Soc.*, **184,** 185.